12-20-2005

The Dust Cloud Around the White Dwarf G29-38

William T. Reach
California Institute of Technology

Ted von Hippel
University of Texas at Austin, vonhippt@erau.edu

et al.

The Astrophysical Journal, 635:L161–L164, 2005 December 20

THE DUST CLOUD AROUND THE WHITE DWARF G29-38

William T. Reach,[1] Marc J. Kuchner,[2] Ted von Hippel,[3] Adam Burrows,[4] Fergal Mullally,[3]
Mukremin Kilic,[3] and D. E. Winget[3]
Received 2005 September 17; accepted 2005 November 11; published 2005 December 7

ABSTRACT

We present new observations of the white dwarf G29-38 with the camera (4.5 and 8 μm), photometer (24 μm), and spectrograph (5.5–14 μm) of the *Spitzer Space Telescope*. This star has an exceptionally large infrared excess, amounting to 3% of the bolometric luminosity. The spectral energy distribution (SED) has a continuum peak around 4.5 μm and a 9–11 μm emission feature 1.25 times brighter than the continuum. A mixture of amorphous olivine and a small amount of forsterite in an emitting region 1–5 $R_{\odot}$ from the star can reproduce the shape of the 9–11 μm feature. The SED also appears to require amorphous carbon to explain the hot continuum. Our new measurements support the idea that a relatively recent disruption of a comet or asteroid created the cloud.

Subject heading: infrared: stars — stars: individual (G29-38, WD 2326+049) — white dwarfs

1. INTRODUCTION

White dwarfs offer a unique view into the properties of planetary systems. A star can retain much of its planetary system as it leaves the main sequence and evolves through the red giant stage. Although the inner ~5 AU of a planetary system may evaporate within the red giant atmosphere, and planets that were in marginally stable orbits may escape during stellar mass loss, most outer planets and even much of the Oort-Cloud-like extremities of planetary systems should persist around white dwarfs (Debes & Sigurdsson 2002).

The white dwarf Giclas 29-38 (WD 2326+049; McCook & Sion 1987; G29-38 hereafter) has garnered intense interest since Zuckerman & Becklin (1987) discovered infrared emission from this object far in excess of the photosphere. The excess emission, confirmed both by ground-based (Tokunaga et al. 1990) and space-based (Chary et al. 1999) observations, begins to deviate from a pure photosphere in the near-infrared. While it was initially speculated that a Jupiter-sized companion could supply all the infrared excess, follow-up observations (e.g., Kuchner et al. 1998; Graham et al. 1990) appear to have ruled this out. The colors measured with ISOCAM suggested that the infrared excess is due to particulate matter rather than a brown dwarf companion (Chary et al. 1999).

Besides strong hydrogen absorption lines, G29-38 has some photospheric metal lines, including Ca II which should rapidly ($<10^4$ yr) sink out of the atmosphere due to gravitational sedimentation (Alcock & Illarionov 1980; Koester et al. 1997; Zuckerman & Reid 1998). Possible explanations for the atmospheric metals and the infrared excess include interstellar medium (ISM) accretion (Dupuis et al. 1993; Koester et al. 1997; Zuckerman & Reid 1998), cometary breakup (Alcock et al. 1986), and asteroid disruption (Jura 2003).

We turned the powerful instruments of the *Spitzer Space Telescope* (Werner et al. 2004) toward G29-38 to measure its brightness from 4.5–24 μm. These observations probably probe a planetary system in a late stage of evolution. G29-38's main-sequence progenitor was probably an A star with mass ~3.1 $M_{\odot}$ (Weidemann 2000), similar to many stars known to have debris disks and potential planetary systems (Rieke et al. 2005). The post-AGB phase age is estimated to be ~5×10^8 yr (Bergeron et al. 1995a).

2. OBSERVATIONS

Figure 1 shows the spectral energy distribution (SED) of G29-38. Observations with the Infrared Array Camera (IRAC; Fazio et al. 2004) were performed on 2004 November 26 10:54 UT. At each of five dithers in a Gaussian spatial distribution, a 30 s frame was taken with the 4.5 and 8 μm arrays. We extracted our photometry using the method (Reach et al. 2005) used for the IRAC calibration stars. The quoted 4.5 and 8 μm fluxes, measured from the basic calibrated data, are 8.8 ± 0.3 and 8.2 ± 0.3 mJy, respectively. We calculated color corrections of 0.995 and 1.17 in the 4.5 and 8 μm channels, respectively, making the estimated fluxes 9.2 and 7.0 mJy at the IRAC nominal wavelengths of 4.493 and 7.782 μm. Observations with the Multiband Imaging Photometer for *Spitzer* (MIPS; Rieke et al. 2004) were performed on 2004 December 2 04:45 UT. Three cycles of small-scale photometry dithers were taken with 10 s frames (total exposure time 420 s); the flux at 24 μm is 2.4 mJy.

Observations with the Infrared Spectrograph (IRS; Houck et al. 2004) were performed on 2004 December 8 3:26 UT. The source was first observed on the blue filter portion of the peak-up array; the flux measured from the 16 μm peak-up image is 3.7 mJy. The spectrum from 5.2 to 14.4 μm was assembled by differencing observations at two nods on each of the four spectral orders. The flux derived from the IRS spectrum convolved with the IRAC 8 μm bandpass is consistent with the IRAC flux.

The IRS spectrum shows continuum emission and a strong 9–11 μm feature characteristic of silicate minerals. It shows none of the bands at 6.2, 7.7, 8.6, 11.3, or 12.6 μm characteristic of polycyclic aromatic hydrocarbons (PAHs) that normally dominate mid-infrared spectra of the ISM. The excess emission above photospheric is approximated by two modified blackbodies with temperatures 890 and 290 K, dilution factors (at 10 μm wavelength) 4.2×10^{-16} and 6.3×10^{-15}, and emissivity proportional to $\nu^{0.5}$. These functions are only intended as mathematical approximations of the continuum shape.

[1] *Spitzer* Science Center, MS 220-6, California Institute of Technology, Pasadena, CA 91125; reach@ipac.caltech.edu.

[2] NASA Goddard Space Flight Center, Greenbelt, MD 20771.

[3] Department of Astronomy, University of Texas, 1 University Station C1400, Austin, TX 78712.

[4] Department of Astronomy and Steward Observatory, University of Arizona, 933 North Cherry Avenue, Tucson, AZ 85721.

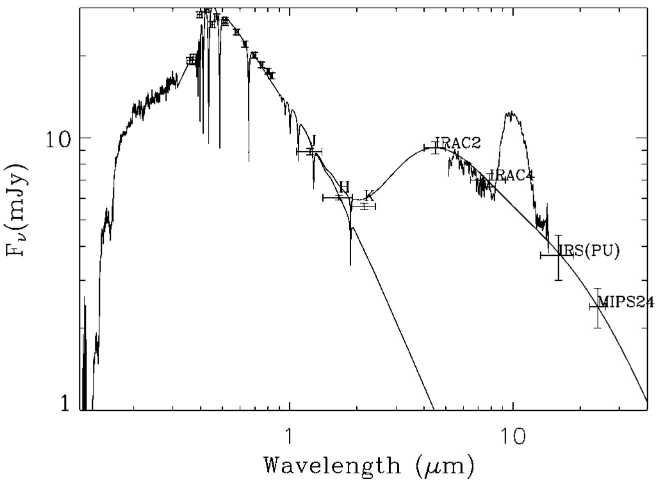

FIG. 1.—SED of the white dwarf G29-38 from the ultraviolet through infrared. The infrared observations are described in § 2, and the ultraviolet through near-infrared observations and model are described in § 3. The solid line through the infrared data is a modified blackbody fit to the continuum.

3. MODELING

We adopt the following basic parameters for G29-38. It is a DA4-type white dwarf, with atmospheric spectrum dominated by H lines (Green et al. 1986). It has an assumed mass of 0.69 $M_\odot$, surface gravity $\log g = 8.14$, and temperature 11,800 K (Bergeron et al. 1995b). The parallax is $\pi = 0''.071 \pm 0''.004$ (Harrington & Dahn 1980), implying a distance of 14 pc.

We assembled the SED from the *International Ultraviolet Explorer* (*IUE*) low-dispersion spectrum covering 0.115–0.3148 μm (Holberg et al. 2003) and a model atmosphere for $T = 12{,}000$ K and $\log g = 8$ covering 0.35–60 μm (D. Koester 2005, private communication). We used the 2MASS photometry ($J = 13.132 \pm 0.029$, $H = 13.075 \pm 0.022$, $K_s = 12.689 \pm 0.029$) and optical spectrophotometry from Palomar (Greenstein & Liebert 1990) for normalization, giving extra weight to the 2MASS *J*-band photometry, the longest wavelength where we think the photosphere dominates. The integrated luminosity of the star is $2 \times 10^{-3}\, L_\odot$.

The 9–11 μm emission feature indicates silicates. Figure 2 compares the shape of the G29-38 silicate feature to that of interstellar dust (Kemper et al. 2004), solar system zodiacal light, the O-rich mass loss from the star Mira (Sloan et al. 2003), and comet Hale-Bopp (C/1995 O1; Crovisier et al. 1997). The G29-38 silicate feature is redder than that of the ISM, which has a single, rounded peak at 9.7 μm and nearly linear slopes on either side. This suggests that the material around G29-38 is not accreted ISM but rather is indigenous to the star. The G29-38 silicate feature is more compact than the zodiacal light silicate feature and than the exozodiacal light feature around β Pic (Reach et al. 2003). The Hale-Bopp spectrum has a prominent 11.3 μm peak that is not seen in the G29-38 spectrum. The Mira silicate feature is somewhat redder and wider than the ISM feature, roughly intermediate between the ISM and G29-38 feature shape. The G29-38 silicate feature shape is most similar to (and approximately intermediate between) those of Mira and the zodiacal light, but the line-to-continuum ratio of G29-38 is much greater than that of the zodiacal light (125% vs. 6%), suggesting a very different particle size distribution.

We computed theoretical emission spectra for grains (size $a = 0.01$–1000 μm, $dn/da \propto a^{-3.5}$) of various compositions

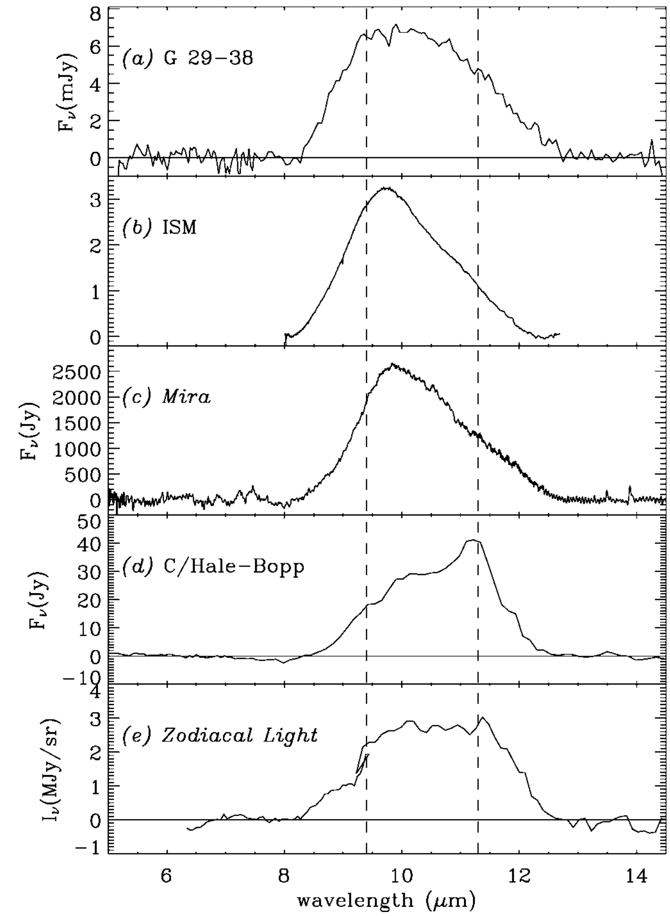

FIG. 2.—Continuum-subtracted spectrum of the silicate feature from G29-39, compared to similarly subtracted silicate features of the diffuse ISM, the O-rich star Mira, comet Hale-Bopp, and the zodiacal light.

(amorphous carbon, crystalline enstatite, amorphous pyroxene [50/50 Mg/Fe], amorphous olivine [50/50] and crystalline forsterite) around G29-38 to further elucidate the properties of the dust around that star. The temperatures and emissivities over a range of distances (0.003–3.5 AU $= 0.6$–$750\, R_\odot$) from the white dwarf were integrated over a spherical, presumed optically thin shell with a radial profile $n \propto r^{-\alpha}$ and an inner cutoff at $R_{\rm min}$. The temperatures of 0.5 μm radius grains of amorphous carbon (olivine) are 600 K (920 K) at 3 $R_\odot$ and 130 K (110 K) at 1 AU from the white dwarf. Grains hotter than 1500 K are presumed to be sublimated and are not included in the emission. Since we assume that the cloud is optically thin, we cannot further constrain the geometry of the emitting region, which could range from a spherical shell to a flattened disk.

The G29-38 silicate feature resembles the amorphous olivine model, with excess on the red side that can be accounted for by mixing in forsterite. Pyroxene cannot contribute significantly to the observed spectrum; its 9–11 μm feature is too blue. Amorphous olivine and fosterite alone cannot explain the spectrum, however, because they cannot emit at 3–6 μm without also producing a 1.6 μm feature that exceeds the near-infrared *H*-band flux. The near-infrared continuum shape at these wavelengths matches the amorphous carbon model. The contrast of the silicate feature demands a particle size distribution that favors small particles, unlike that of interplanetary dust grains (Grün et al. 1985). On the assumption that all the particles participate in the same collisional evolution, we assume that silicate and carbon particles share the same size distribution.

The distance of the emitting region from the star is constrained as follows. In order to produce significant emission at 5 μm, we require $R_{\min} < 5\ R_{\odot}$. The best-fitting models all require small $R_{\min}$, implying that the dust exists nearly up to its sublimation temperature. The radial profile shape requires high α, suggesting that the emitting region extends from 1 to 10 $R_{\odot}$ from the star. Figure 3 shows the observed spectrum and the best-fit model. Experiments with other geometries yielded similar results: a face-on slab required $\alpha \sim 3$, $R_{\min} \sim 2.5\ R_{\odot}$. A dust cloud this small is consistent with the measurements of Kuchner et al. (1998), which showed G29-38 to be unresolved in the *K* band at 55 mas (160 $R_{\odot}$) resolution.

4. CONCLUSIONS

A cloud of small grains 1–10 $R_{\odot}$ from G29-38 creates its mid-infrared emission. The luminosity of the infrared excess is 3% of the luminosity of the star, high by the standards of debris disks, indicating nontrivial disk opacity in the ultraviolet–visible range.

Our models suggest a dust grain abundance ratio (by number) of olivine : carbon : forsterite of 5 : 12 : 2. Considering only the atoms in these grains, assuming material densities of 2.2 and 2.5 g cm^{-3} for the amorphous carbon and silicates, the abundance ratio (by number) of C : O is 3 : 1. The total dust mass required to generate the observed mid-infrared flux is of the order of 10^{18} g; a larger mass could be present if there are larger, cooler grains that do not contribute to the observed flux. This inferred mass corresponds to that of a ~10 km diameter asteroid or comet, and is slightly less than the mass of the interplanetary dust responsible for the zodiacal light in the solar system (Fixsen & Dwek 2002).

Where could this dust cloud have come from? It was not generated by the white dwarf (by any known mechanism), nor is it likely to be planetary system material that was at this location before the star was a red giant, whose atmosphere would have extended much further than the current dust cloud. The silicate feature is suggestive of dust formed in O-rich mass loss during the red giant or AGB phase, but the presence of significant and comparable amounts of silicate and carbonaceous dust (and no PAH) does not seem compatible with such dust, which in any event could not have survived at 10 $R_{\odot}$ from the star. The material must have been transported inward. If the material originates from the planetary system of the progenitor, then gravitational perturbations would occasionally send smaller bodies close to the star. If the small body is collisionally fragmented, loses mass by cometary sublimation, or breaks apart by thermal or gravitational stress, the Poynting-Robertson effect will cause particles of radius *a* (μm) and distance *r* ($R_{\odot}$) to spiral into the star on timescales of $4r^2a$ yr, i.e., a few years for material contributing to the mid-infrared emission. The particles would continue toward the star until they sublimate, suffer mutual collisions, and disrupt, with part of the material landing in the photosphere, part being blown out of the system by radiation pressure, and part remaining on bound orbits. If the entire mid-infrared–emitting mass (i.e., particles out to ~10 $R_{\odot}$) were lost in the Poynting-Robertson timescale, the accretion rate is of the order of 10^{15} g yr^{-1}. This flow could be supplied by collisional comminution of debris from an asteroidal and cometary cloud like the one in the solar system (Sykes & Greenberg 1986). This mass-loss rate is comparable to the "high" ISM accretion scenario calculated by Dupuis et al. (1993), which appears inconsistent with G29-38's present location in a low-density ISM environment.

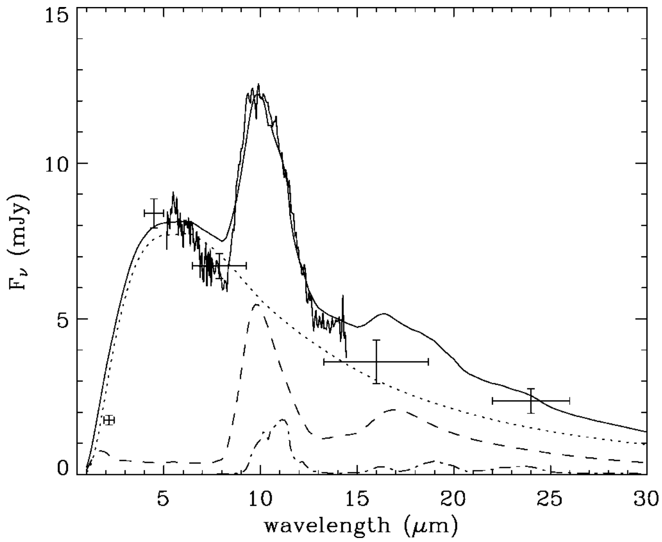

FIG. 3.—Infrared excess of G29-38 compared to the best-fit model (*solid line*), consisting of three compositions: amorphous carbon (*dotted line*), amorphous olivine (*long-dashed line*), and forsterite (*dot-dashed line*).

A plausible model for the infrared excess around G29-38 involves the tidal disruption of an asteroid near the white dwarf (Graham et al. 1990; Jura 2003). Since short-period comets are composed largely of refractory material, we generalize this model to include the tidal disruption of a comet. Comets are commonly observed to pass near the Sun, so by analogy a surviving reservoir of comets (and possibly a surviving massive outer planet) would inevitably lead to star-grazing cometary passages. With its low luminosity, the white dwarf would not drive a high sublimation rate for star-grazing comets, reducing the related stresses that appear to cause Sun-grazing comets to split. Comets may then travel rather close to the white dwarf, where they could be disrupted by tidal forces. Our new observations support this model, since the emitting region lies close to the star, where a large solid body would be tidally disrupted. Based on the high C/O ratio in the dust, it is also conceivable that the "comet" was condensed out of the AGB mass loss (Kuchner & Saeger 2005). The details of the tidal disruption model presented here are different from those in previous papers, which assume larger grains and an optically thick disk. If the emitting region is a disk, it is either optically thin or viewed relatively face-on, with the line of sight from the white dwarf to the Sun relatively free of dust. For a thin disk to absorb 3% of the luminosity of the star it would have to be opaque in the ultraviolet, where there is no evidence of significant extinction and no 2175 Å absorption bump in the *IUE* spectrum.

An alternate and long-standing model for both the photospheric metals and the infrared excess is dredge-up and mass loss. There are already difficulties with dredge-up models associated with the need for vertical velocities that are at odds with G29-38's *g*-mode pulsations that are overwhelmingly horizontal. Furthermore, standard white dwarf models are layered from prior nuclear burning; hypothetical mixing from the pulsations would have to reach many orders of magnitude below the convection zone boundary, well below even the degeneracy boundary (~$10^{-6}\ M_{\odot}$) to dredge up material from the C/O layer (presumably around $10^{-3}\ M_{\odot}$ or deeper). Furthermore, the dredge-up hypothesis cannot explain the abundant silicates; invoking these materials just below the He layer is very difficult to accommodate within our current understanding of nuclear burning of He in post–main-sequence stars appropriate to white dwarf stars in the mass range of G29-38. Our observations therefore argue that the observed material was not formed in the white dwarf, but formed well outside its current position.

The presence of a dust cloud around G29-38 is likely related to the anomalous presence of metals in its photosphere. As discussed by Zuckerman et al. (2003), the photospheric metals could be accreted from interstellar gas, but then the star would need to be within a dense cloud (because the lifetime of metals in the photosphere [$<10^4$ yr] is smaller than the crossing time of a dense cloud [$\gtrsim 10^4$ yr]), which is not true for G29-38. The other major model for white dwarf photospheric metals is cometary impact (Zuckerman & Reid 1998; Debes & Sigurdsson 2002). On the basis of the presence of a strong silicate feature and the overall mid-infrared SED, we believe this latter model prevails for G29-38.

The abundance of photospheric metals for G29-38 is among the highest of any known for a white dwarf, and the infrared excess is also the highest of any known white dwarf. Another white dwarf, WD 1337+705 (G238-44), with even higher atmospheric Ca abundance (Zuckerman et al. 2003), does not show infrared excess at the level seen in G29-38 in our *Spitzer* photometric survey of white dwarfs at 4.5 and 8 μm. It is possible that a recent disruption of an asteroid or comet has occurred in G29-38, repopulating the star's dust cloud at a level much higher than the long-term steady state, as indeed occurs in debris disks around main-sequence stars (Rieke et al. 2005) and the solar system (Sykes & Greenberg 1986).

Are there planets around G39-38? The 9–11 μm spectral feature proves that there is a cloud of small silicate grains. We ascribed the 3–6 μm continuum to amorphous carbon dust, and the carbon-silicate mix matches the SED, but there is no spectral signature for carbon other than its color temperature. If we ascribe the 890 K continuum to a planet, then it must be not only very hot but also very large, with radius 0.2 $R_\odot$—an extremely unusual object. If the dust cloud is indeed due to an asteroid or comet, perhaps other, cooler planets await discovery around the fascinating star G29-38.

This work is based in part on observations made with the *Spitzer Space Telescope*, which is operated by the Jet Propulsion Laboratory, California Institute of Technology under NASA contract 1407. Support for this work was provided by NASA through award project NBR 1269551 issued by JPL/Caltech to the University of Texas.

REFERENCES

Alcock, C., Fristrom, C. C., & Siegelman, R. 1986, ApJ, 302, 462
Alcock, C., & Illarionov, A. 1980, ApJ, 235, 534
Bergeron, P., Wesemael, F., & Beauchamp, A. 1995a, PASP, 107, 1047
Bergeron, P., Wesemael, F., Lamontagne, R., Fontaine, G., Saffer, R. A., & Allard, N. F. 1995b, ApJ, 449, 258
Chary, R., Zuckerman, B., & Becklin, E. E. 1999, in The Universe as Seen by *ISO*, ed. P. Cox & M. F. Kessler (ESA-SP 427; Garching: ESA), 289
Crovisier, J., Leech, K., Bockelee-Morvan, D., Brooke, T. Y., Hanner, M. S., Altieri, B., Keller, H. U., & Lellouch, E. 1997, Science, 275, 1904
Debes, J. H., & Sigurdsson, S. 2002, ApJ, 572, 556
Dupuis, J., Fontaine, G., & Wesemael, F. 1993, ApJS, 87, 345
Fazio, G. G., et al. 2004, ApJS, 154, 10
Fixsen, D. J., & Dwek, E. 2002, ApJ, 578, 1009
Graham, J. R., Matthews, K., Neugebauer, G., & Soifer, B. T. 1990, ApJ, 357, 216
Green, R. F., Schmidt, M., & Liebert, J. 1986, ApJS, 61, 305
Greenstein, J. L., & Liebert, J. W. 1990, ApJ, 360, 662
Grün, E., Zook, H. A., Fechtig, H., & Giese, R. H. 1985, Icarus, 62, 244
Harrington, R. S., & Dahn, C. C. 1980, AJ, 85, 454
Holberg, J. B., Barstow, M. A., & Burleigh, M. R. 2003, ApJS, 147, 145
Houck, J. R., et al. 2004, ApJS, 154, 18
Jura, M. 2003, ApJ, 584, L91
Kemper, F., Vriend, W. J., & Tielens, A. G. G. M. 2004, ApJ, 609, 826
Koester, D., Provencal, J., & Shipman, H. L. 1997, A&A, 320, L57
Kuchner, M. J., Koresko, C. D., & Brown, M. E. 1998, ApJ, 508, L81
Kuchner, M. J., & Saeger, S. 2005, ApJ, submitted
McCook, G. P., & Sion, E. M. 1987, ApJS, 65, 603
Reach, W. T., Morris, P., Boulanger, F., & Okumura, K. 2003, Icarus, 164, 384
Reach, W. T., et al. 2005, PASP, 117, 978
Rieke, G. H., et al. 2004, ApJS, 154, 25
———. 2005, ApJ, 620, 1010
Sloan, G. C., Kraemer, K. E., Price, S. D., & Shipman, R. F. 2003, ApJS, 147, 379
Sykes, M. V., & Greenberg, R. 1986, Icarus, 65, 51
Tokunaga, A. T., Becklin, E. E., & Zukerman, B. 1990, ApJ, 358, L21
Weidemann, V. 2000, A&A, 363, 647
Werner, M. W., et al. 2004, ApJS, 154, 1
Zuckerman, B., & Becklin, E. E. 1987, Nature, 330, 138
Zuckerman, B., Koester, D., Reid, I. N., & Hünsch, M. 2003, ApJ, 596, 477
Zuckerman, B., & Reid, I. N. 1998, ApJ, 505, L143